$L1_0$-ordered FePtAg–C granular thin film for thermally assisted magnetic recording media (invited)

L. Zhang,[1,a] Y. K. Takahashi,[1] K. Hono,[1] B. C. Stipe,[2] J.-Y. Juang,[2] and M. Grobis[2]
[1]*Magnetic Materials Center, National Institute for Materials Science, 1-2-1 Sengen, Tsukuba 305-0047, Japan*
[2]*Hitachi Global Storage Technologies, San Jose Research Center, San Jose, California 95135, USA*

(Presented 15 November 2010; received 23 September 2010; accepted 3 November 2010; published online 17 March 2011)

We studied highly $L1_0$-ordered FePtAg–C nanogranular film as a potential high-density storage medium in thermally assisted magnetic recording (TAR). A 6.4-nm-thick FePtAg–C film with a perpendicular coercivity of 37 kOe and an average grain size of 6.1 ± 1.8 nm was fabricated on oxidized silicon substrate with a 10 nm MgO interlayer at 450 °C. The time-dependence measurement of remnant coercivity showed the energy barrier of $E_b = 7.6$ eV $\sim 300\ k_BT$ at room temperature, meaning the excellent thermal stability for long-term data storage. Static tester experiments on this film using a TAR head demonstrate the feasibility of recording at an areal density of ~450 Gbits/in.^{2}. © *2011 American Institute of Physics*. [doi:10.1063/1.3536794]

I. INTRODUCTION

$L1_0$-ordered FePt granular thin films are considered as the most promising candidates for perpendicular magnetic recording (PMR) media for recording densities exceeding 1 Tbits/in.^{2} because the high magnetocrystalline anisotropy ($K_u \sim 7 \times 10^7$ ergs/cm^3) of the $L1_0$ FePt phase allows one to reduce the grain size to as small as 4 nm without thermal instability of magnetization.[1–3] The difficulty of switching the magnetization of high coercivity single domain $L1_0$-FePt particles can be overcome by the thermally assisted magnetic recording (TAR) process.[4–7] For the practical application of FePt films as a TAR media, the *c*-axis of magnetically isolated $L1_0$-FePt particles of less than 5 nm with a size distribution of less than 1.0 nm must be perfectly aligned to the normal direction to the film plane. In addition, appropriate thermal conductance of the underlayers and substrate will be necessary. In our early effort, we succeeded in fabricating well-separated perpendicular anisotropic granular films with a narrow size distribution by cosputtering FePt and C on a MgO interlayer.[8] The polycrystalline MgO layer grew with strong (001) texture on thermally oxidized silicon substrates, which worked as an effective seed layer for the epitaxial growth of (001) FePt particles. Nevertheless, the coercivity of the FePt–C films was only 10 kOe at the substrate temperature of 450 °C. To increase the coercivity by enhancing the $L1_0$ ordering, we introduced Ag into the FePt–C granular thin films, and succeeded in the fabrication of high coercivity (37 kOe) FePtAg–C granular films with perpendicular anisotropy.[9] However, there was no report on the TAR demonstration on the FePt granular films. In this paper, we have studied the thermal stability of the FePtAg–C granular thin films and performed static tester measurements on this granular film using a TAR head to demonstrate that high density thermally assisted recording is possible using the FePtAg–C granular films.

[a]Author to whom correspondence should be addressed. Electronic mail: Zhang.Li@nims.go.jp.

II. EXPERIMENTAL PROCEDURES

First, a MgO layer was deposited on a thermally oxidized silicon substrate at 100 °C by rf sputtering under 1.3 Pa Ar gas pressure with a deposition rate of 0.033 nm/s. A $Fe_{0.49}Pt_{0.41}Ag_{0.1}$–50 vol. % C film was deposited by cosputtering Fe, Pt, Ag, and C in an ultrahigh vacuum magnetron and rf sputtering machine on the predeposited MgO layer at 450 °C under 0.3 Pa Ar with a deposition rate of 0.02 nm/s.[9] The thickness of the film and the atomic fraction of Fe, Pt, Ag, and C were estimated based on the precalibrated sputtering rates of the above-mentioned elements, respectively. For each element grown separately on the silicon wafer, after checking the thickness of the film, we converted the thickness or volume of the film into the mole amount of atoms based on its molecular mass and density values. In this way, we are able to get the atomic ratio of Fe, Pt, and Ag in the film, with an error of <1%. Note that the Fe:Pt ratio in this film was 54:46, not 50:50, for achieving the best $L1_0$ order in the film. This is consistent with other researchers' work on $L1_0$-ordered FePt thin films.[10–12] The crystalline structure and the $L1_0$ ordering of the film were examined by the standard x-ray diffraction (XRD) technique using the Cu $K\alpha$ radiation. The magnetic properties were measured with a Quantum Design MPMS superconducting quantum interferometer device (SQUID) with an applied magnetic field of up to ±55 kOe. The structure of the film was characterized by the standard XRD and transmission electron microscopy (TEM) using FEI Technai 20 and F30 TEMs.

An antenna-integrated TAR head was used to demonstrate the recording process on this FePt thin film in a static tester.[13,14] In the design of the TAR head, we integrated a Ta_2O_5 waveguide core with a uniform rectangular cross section surrounded by low index cladding layers to guide light from the top of the recording head to near the air-bearing surface. A plasmonic antenna was fabricated at the end of the waveguide. The write pole of the head was designed to provide a magnetic field without significantly reducing the optical efficiency of the head. When the pulsed laser light

reaches the plasmonic antenna, it creates an intense optical pattern in the near field, heating the disk at the nanometer scale. This writing technique allows one to use extremely high anisotropy media (such as $L1_0$-FePt) for reduced grain size while maintaining the requirements of thermal stability and writability. Light from an external diode laser at 830 nm wavelength was focused and end-fired into the top of the waveguide. Integrated heads were mounted on head gimbal assembly and recording was carried out in a quasistatic tester. Nanosecond laser pulses and pulsed magnetic field from the write pole were applied for static tester recording experiments. Images were generated by scanning the onboard tunneling magnetoresistive (TMR) element (70 nm width), or the TMR element from a second head (narrower width).

III. RESULTS AND DISCUSSION

Figure 1 shows the TEM bright-field image, selected area electron diffraction (SAED) pattern, and grain size distribution of the film.[9] Both XRD and SAED results display distinct (001) superlattice reflection and the (002) fundamental reflection of the $L1_0$-FePt particles. The $(200)_{MgO}$ ring suggests that the polycrystalline MgO interlayer is strongly (100) textured. The missing $(111)_{FePt}$ diffraction ring suggests that the $L1_0$-FePt crystals are also strongly (001) textured. In the bright-field TEM image, FePt particles are observed with a darker contrast, although the contrast varies depending on the diffraction conditions arising from slight changes in orientation. Our previous energy-filtered TEM images indicated that Ag is dissolved in the FePt particles, whereas C forms intergranular phase to isolate FePtAg particles.[9] The brightly imaging channels are amorphous carbon. The average grain size of the film was determined to be 6.1 ± 1.8 nm. The average value of center-to-center distance was measured to be 9.6 nm from the TEM bright-field image so that the average carbon spacing is estimated to be 3.5 nm or less (it could be overestimated as it ignores the volume of the triple points). Figure 2

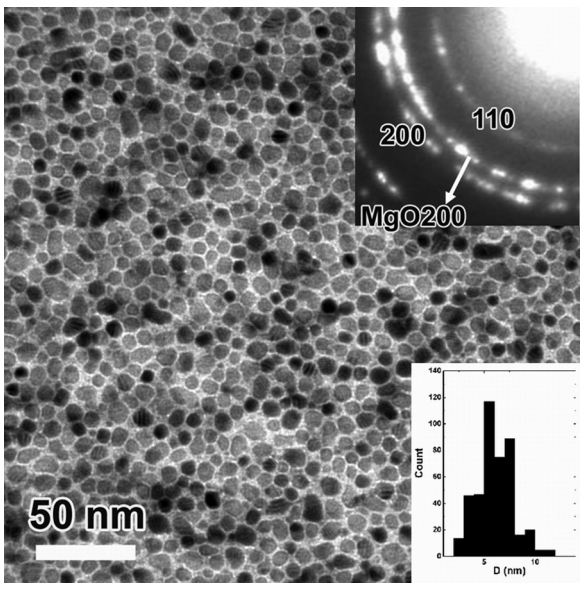

FIG. 1. TEM bright-field image, SAED pattern, and grain size distribution diagram of the FePtAg–C granular film.

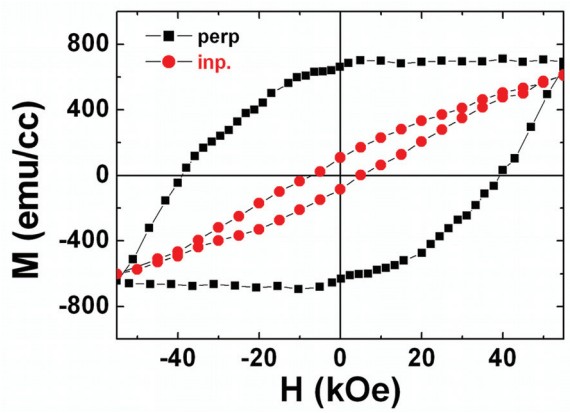

FIG. 2. (Color online) Both perpendicular and in-plane *M–H* loops of the FePtAg–C granular film.

shows magnetization curves in both perpendicular and in-plane directions to the film plane. The *M–H* loops show that this film has a perpendicular coercivity of 37 kOe, and in-plane 5 kOe, respectively. Note that the perpendicular *M–H* loop may not be fully saturated in the maximum field of 55 kOe from SQUID, the actual coercivity value could be even higher than 37 kOe. It indicates that the *c*-axis of this film is predominantly normal to the film plane. The anisotropy K_u of this film was estimated to be 4.2×10^7 ergs/cm^3 from the *M–H* loops.[9]

Next, we study the thermal stability of this granular film. In order to estimate its energy barrier, E_b, we measured the time dependence of remnant coercivity described by the Scharrock equation,[15,16]

$$H_c(t) = H_{c0}\left\{1 - \left[\frac{k_B T}{E_b}\ln\left(\frac{f_0 t}{0.693}\right)\right]^{1/2}\right\}, \qquad (1)$$

where $H_c(t)$ is defined as the remnant coercivity, the field that switches half of the particles in the sample in the field duration of t, f_0 is called the attempt frequency, with a typical value of 10^9 Hz for magnetic system,[3] and $k_B T$ represents the thermal energy required to flip the magnetization, causing the thermal decay of the magnetic system. The assumption of the Scharrock equation is that the magnetization switching occurs by the coherent rotation. The average particle diameter of our granular film is 6.1 nm with the thickness of 6.4 nm. From a theoretical model by Li et al,[10] we estimated the size of a single FePt domain to be ~15 nm for this film. Thus, all the particles in the film are considered to be single domain, satisfying the assumption of the Scharrock equation. In normal measurement of perpendicular *M–H* loops by SQUID, the waiting time at each data point is ~1 s after the application and stabilization of the magnetic field. In order to observe the magnetic decay, the waiting time was increased and varied from 10 to 1000 s in this experiment. First, we applied a huge positive field +55 kOe; then the field was reduced to negative from −31 to −43 kOe fields around the coercive point for some waiting time *t*; after that we set the field to zero, and measure the magnetic moment of the film. Figure 3(a) shows the magnetization vs field, displaying a distinct decay with increasing time. For

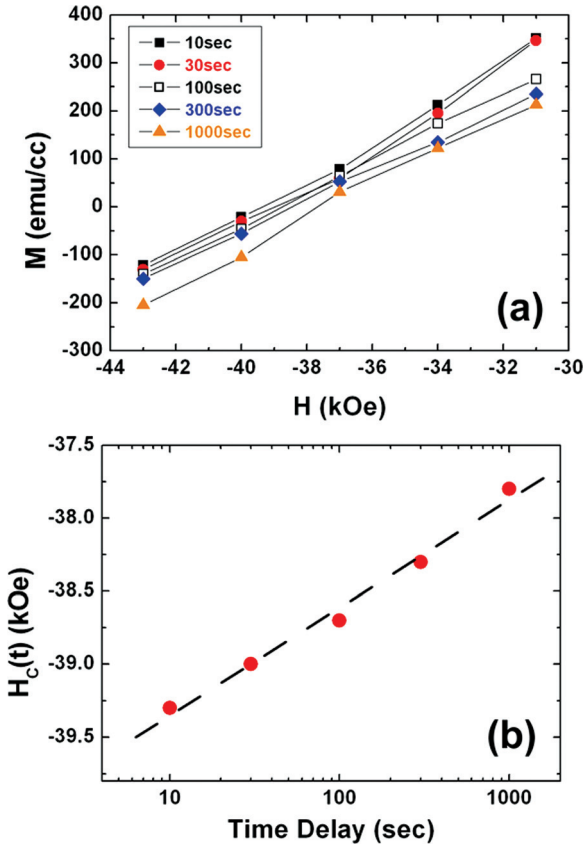

FIG. 3. (Color online) (a) The magnetization measured at different field with various decay time and (b) the remnant coercivity vs time delay.

each time t, we apply linear fitting for the $M(H)$ curve, and then get the remnant coercivity at zero field. The plot was displayed in Fig. 3(b). By fitting through Eq. (1), we obtained $E_b = 7.6$ eV, and $H_{c0} = 43.5$ kOe. At room temperature $T = 300$ K, $k_BT = 0.025$ eV, so $E_b \sim 300\ k_BT$. Note that the typical E_b for the current recording media using CoCrPt-based alloys is around 80 k_BT. Therefore, this $L1_0$-FePt granular film has excellent thermal stability, much better than current CoCrPt media. Note also that the E_b value estimated from K_uV is approximately 92 k_BT at room temperature, using $K_u = 4.2 \times 10^7$ ergs/cm^3 and $V = 9.5 \times 10^{-21}$ cm^3. In the latter model, we simply neglected magnetostatic and exchange interactions among adjacent grains, and assume that the grain is a completely isolated Stoner-Wohlfarth (SW) particle.[17] However, the Sharrock model originally described the magnetic switching behavior of an isolated SW particle without any interaction among particles. When it was applied to the magnetic system with a huge amount of particles the switching volume (described in $E_b = K_uV^*$) may not be consistent with the actual volume V viewed from the microstructure.

Figure 4 shows the recording pattern tracks written at bit lengths of 40 and 20 nm at a track width of 85 nm. The signal-to-noise ratio (SNR) was determined by the center-track scan lines of the image. We compare the SNR of the FePt-TAR tones to the SNR obtained on well-characterized conventional head and PMR media using the static tester. Using the measured 1 T SNR of the conventional recording system as benchmark, we found that the 20 nm tone on FePt media

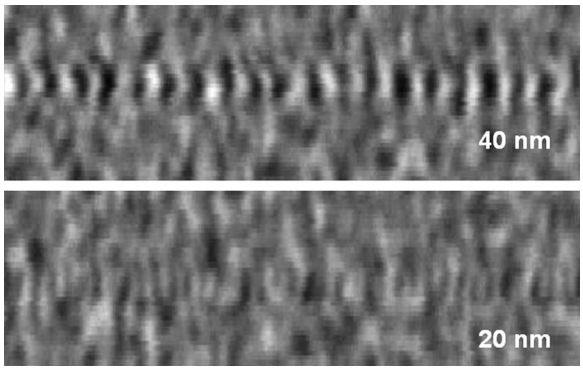

FIG. 4. Recording pattern tracks written at bit lengths of 40 and 20 nm, the track width is 85 nm.

has a higher SNR value. By performing SNR measurements at different bit pitches, we estimate that the SNR on this FePt medium matches the 1 T SNR of the conventional recording system at a bit pitch of 17 nm. Taking the narrow-band amplitude full-width at half-maximum (FWHM) of the tracks as an estimation of the achievable track pitch and 17 nm as the smallest achievable bit length, we calculate the achievable areal density as 450 Gbits/in.^{2} Actual areal density at sufficiently low error rate for commercialization may be somewhat lower or higher than this estimation.

In Fig. 5, we show (a) the read-back pattern tracks by a 40-nm-wide TMR head, and together with (b) a cross-track scan of TAR tracks written at successively higher laser powers with a 50 nm bit length. Shown in Fig. 5, the track width FWHM, as measured by the reader, was 60, 74, 97, and 125 nm for wave guide optical powers at 17, 21, 25, and

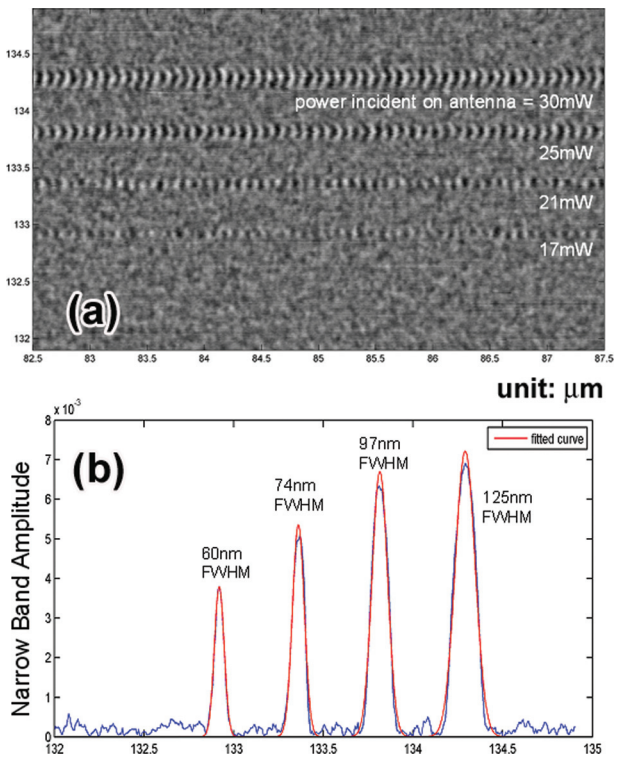

FIG. 5. (Color online) (a) Read-back pattern tracks with 40-nm-wide TMR head and (b) cross-track scan of TAR tracks written at successively higher laser powers with 50 nm bit length.

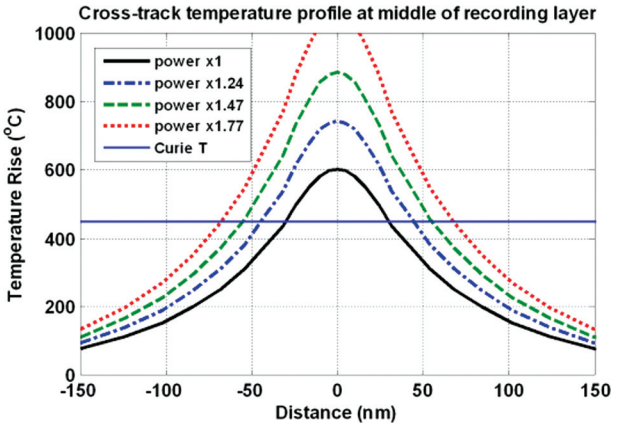

FIG. 6. (Color online) Cross-track temperature profile at the middle of the recording layer as a function of absorption power. The track widths are 60, 88, 110, and 134 nm for normalized absorption power of 1, 1.24, 1.47, and 1.77, respectively. The writing is assumed to occur at Curie temperature of 450 °C for recording medium.

30 mW, respectively. We found that a 60 nm track width was measured near the threshold. Because the FePtAg–C thin film was fabricated on a silicon substrate with excellent thermal conductivity, this film displays efficient heat-sinking and can support a 60 nm track width with a good signal. Meanwhile, we are aware that this silicon substrate was coated with an amorphous SiO_2 layer of ~120 nm in thickness. Since the bit size is expected to be influenced by the volume of heated zones, the reduction in the thickness of the a-SiO_2 layer may lead to further reduction of the thermal spot size. If a naturally oxidized silicon substrate is used, better thermal conductance may be achieved. The influence of the thermal conductance of substrates will be the subject for the next stage of TAR recording media.

To illustrate the temperature distribution in the recording layer, we first obtained a three-dimensional optical absorption profile in the media using a finite-element time-domain simulator (EMFLEX, Weidlinger Associates Inc.), and then calculated the temperature profile with the absorption power as a heat source by a finite-element method. The model includes the detailed structure of each layer on the substrate. The thermal boundary resistance between the FePtAg–C and MgO layers was included with an interface thermal conductance of 700 MW/m^2 K.[18] The linear velocity of the FePtAg–C recording film relative to the laser spot was chosen to be 8 m/s, a typical value in current hard disk drive systems. During the transient heat transfer process, the peak temperature value was recorded at the time when heating is finished. The cross-track temperature profile at the middle of recording layer as a function of absorption power is shown in Fig. 6. The track width was estimated to be 60, 88, 110, and 134 nm for the normalized absorption power of 1, 1.24, 1.47, and 1.77, respectively, assuming the writing occurs near the Curie temperature of the FePt, $T_C = 450$ °C.[19,20] The sensitivity of track width to power correlates well with the FWHM of the narrowband amplitude measurement in Fig. 5(b).

IV. CONCLUSION

We studied highly $L1_0$-ordered FePtAg–C nanogranular film as a potential high-density storage medium in thermally assisted magnetic recording (TAR). A 6.4-nm-thick FePtAg–C film with the perpendicular coercivity of 37 kOe and average grain size of 6.1 ± 1.8 nm was fabricated on an oxidized silicon substrate with a 10 nm MgO interlayer at 450 °C. The time-dependence measurement of remnant coercivity showed the energy barrier of $E_b = 7.6$ eV~300 k_BT at room temperature, meaning the excellent thermal stability for long term data storage. Static tester experiments on this film using a TAR head demonstrate the feasibility of recording at an areal density of approximately 450 $Gbits/in.^2$ This is encouraging to support the feasibility of applying FePtAg–C granular films to the next generation high density magnetic recording media.

ACKNOWLEDGMENTS

This work was in part supported by World Premier International Research Center Initiative (WPI Initiative) on Materials Nanoarchitronics, MEXT, Japan, Information Storage Industry Consortium (INSIC), and the NEDO project on the Development of Nanobit Technology for Ultra-High Density Magnetic Recording Project (Green IT Project).

[1] J.-U. Thiele, L. Folks, M. F. Toney, and D. K. Weller, J. Appl. Phys. **84**, 5686 (1998).
[2] M. L. Yan, X. Z. Li, L. Gao, S. H. Liou, D. J. Sellmyer, R. J. M. van de Veerdonk, and K. W. Wierman, Appl. Phys. Lett. **83**, 3332 (2003).
[3] P. L. Lu, and S. H. Charap, IEEE Trans. Magn. **31**, 2767 (1995).
[4] J. J. M. Ruigrok, R. Coehoorn, S. R. Cumpson, and H. W. Kesteren, J. Appl. Phys. **87**, 5398 (2000).
[5] M. Alex, A. Tselikov, T. McDaniel, N. Deeman, T. Valet, and D. Chen, IEEE Trans. Magn. **37**, 1244 (2001).
[6] M. Mochida, M. Birukawa, and T. Suzuki, IEEE Trans. Magn. **37**, 1396 (2001).
[7] W. A. Challener, C. Peng, A. V. Itagi, D. Karns, W. Peng, Y. Peng, X. Yang, X. Zhu, N. J. Gokemeijer, Y.-T. Hsia, G. Ju, R. E. Rottmayer, M. A. Seigler, and E. C. Gage, Nature Photon. **3**, 220 (2009).
[8] A. Perumal, Y. K. Takahashi, and K. Hono, Appl. Phys. Exp. **1**, 101301 (2008).
[9] L. Zhang, Y. K. Takahashi, A. Perumal, and K. Hono, J. Magn. Magn. Mater. **322**, 2658 (2010).
[10] G. Q. Li, H. Takahoshi, H. Ito, H. Saito, S. Ishio, T. Shima, and K. Takanashi, J. Appl. Phys. **94**, 5672 (2003).
[11] F. Casoli, F. Albertini, L. Nasi, S. Fabbrici, R. Cabassi, F. Bolzoni, and C. Bocchi, Appl. Phys. Lett. **92**, 142506 (2008).
[12] C. Feng, Q. Zhan, B. Li, J. Teng, M. Li, Y. Jiang, and G. Yu, Appl. Phys. Lett. **93**, 152513 (2008).
[13] B. C. Stipe, T. C. Strand, C. C. Poon, H. Balamane, T. D. Boone, J. A. Katine, J. L. Li, V. Rawat, H. Nemoto, A. Hirotsune, O. Hellwig, R. Ruiz, E. Dobisz, D. S. Kercher, N. Robertson, T. R. Albrecht, and B. D. Terris, Nature Photon. **4**, 484 (2010).
[14] A. Hirotsune, H. Nemoto, I. Takekuma, K. Nakamura, T. Ichihara, and B. C. Stipe, IEEE Trans. Magn. **46**, 1569 (2009).
[15] M. P. Sharrock, J. Appl. Phys. **76**, 6413 (1994).
[16] Y. K. Takahashi, K. Hono, S. Okamoto, and O. Kitakami, J. Appl. Phys. **100**, 074305 (2006).
[17] E. C. Stoner, and E. P. Wohlfarth, IEEE Trans. Magn. **27**, 3475 (1991).
[18] R. M. Costescu, M. A. Wall, and D. G. Cahill, Phys. Rev. B **67**, 054302 (2003).
[19] S. Okamoto, N. Nikuchi, O. Kitakami, T. Miyazaki, and Y. Shimada, Phys. Rev. B **66**, 024413 (2002).
[20] K. Barmak, J. Kim, D. C. Berry, W. N. Hanani, K. Wierman, E. B. Svedberg, and J. K. Howard, J. Appl. Phys. **97**, 024902 (2005).